Power Deposition in a Spherical Model of Man Exposed to 1–20-MHz Electromagnetic Fields

JAMES C. LIN, MEMBER, IEEE, ARTHUR W. GUY, MEMBER, IEEE, AND CURTIS C. JOHNSON, SENIOR MEMBER, IEEE

Abstract—**The induced fields and the associated power deposition in man exposed to HF electromagnetic (EM) fields have been investigated theoretically using spherical models. The induced electric fields inside the model exposed to either plane wave or near fields can be described adequately by a combination of quasi-static electric and magnetic induction solutions. It is shown that for field impedances less than $1200\pi\ \Omega$ the magnetically induced energy absorption predominates. Therefore, H fields must be measured to obtain any estimate of the hazards due to HF exposure.**

For a 70-kg model of man exposed to a plane wave field, the theory indicates that the time-average power absorption per unit volume is less than 2.5×10^{-3} mW/g for each milliwatt per square centimeter incident at 20 MHz and below. This suggests that the thermal safe-exposure levels for the HF band are many orders of magnitude in excess of the 10-mW/cm² level recommended for the microwave region.

Introduction

THE biological effects and potential hazards of electromagnetic (EM) radiation have received considerable attention in recent years [1]–[6]. This is not only because of the increase in the intensity of radio frequency environment as a result of higher power sources and radiation efficiency, but also due to the rapid proliferation of EM devices in homes, industrial plants, and military installations, as well as in health-care facilities. A great deal of research has emphasized the effects of mirowaves on the physiology, biochemistry, and behavior of animal subjects and human beings. However, very little information is available in the published literature regarding the absorption characteristics and mechanism of power deposition into the human body and the subsequent biological effects of HF fields and below.

In order to assess the environmental impact and health implications of HF transmitters in man, one must be able to quantitatively describe the EM field and power deposition in the tissues. The human body is a very complex geometrical structure; thus it is extremely difficult to obtain exact theoretical and/or experimental descriptions. It is desirable to obtain simple analytic expressions which can be used to predict the nature and degree of power deposition in man as a function of body size and shape, source frequency, and field type. The consideration of field type is important since HF transmitting antennas produce intense fields in the immediate locale. Under such near-field conditions, it is known that electric and magnetic fields are out of time phase and the value of the field impedance E/H is influenced by the induction components of the field. Some attempts have been made in the past to investigate the first-order size and wavelength dependences by considering an HF-plane wave incident on a spherical model equivalent in volume to the human body [9], [10]. However, as oversimplified as these studies are, they have suffered from even further oversimplification by considering only electric-field coupling to the lossy dielectric sphere, thereby reducing the usefulness, if not the validity, of their results.

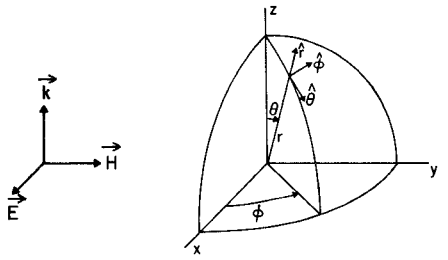

Fig. 1. Spherical coordinate system.

In this report, a tractable first-order size approximation to the problem of HF interaction with the human body is presented using a homogeneous sphere of tissue placed in a plane wave field taking both electric and magnetic fields into consideration. It hardly needs mentioning that the human body is far from spherical, and cylinders and prolate spheroids serve much better as approximating shapes. However, the results and conclusions are not critically dependent on the chosen shape and the simpler shape is chosen in the interest of simple mathematics. This model can be used to obtain first quantitative estimates of the effect of body volume on total EM power absorption and the internal distribution of the absorbed power. The simple closed form expressions provide an easy avenue for realizing the physical significance of the complex mathematical manipulations. It also makes it possible to infer the effect of absorbed power other than plane wave fields with arbitrary field impedance.

Analytical Solution to Mie Equation

Using the spherical coordinate system shown in Fig. 1, Stratton [11] obtained, for a plane wave propagating in the z direction and E polarized in the x direction, the induced electric field in a spherical dielectric

$$E_t = E_0 e^{-i\omega t} \sum_{n=1}^{\infty} i^n \frac{2n+1}{n(n+1)} \left[a_n{}^t m_{o1n}{}^{(1)} - i b_n{}^t n_{e1n}{}^{(1)} \right] \quad (1)$$

with

Manuscript received April 16, 1973; revised August 2, 1973. This work was supported in part by the Aerospace Medical Division, Brooks Air Force Base, Texas, under Contract F41609-73-C-0002, in part by the Social and Rehabilitation Services under Grant 16-P-5618/0–11, and in part by the National Institute of Health under Grant GM 16436.

J. C. Lin and A. W. Guy are with the Department of Rehabilitation Medicine, University of Washington School of Medicine, Seattle, Wash. 98195.

C. C. Johnson was with the Center for Bioengineering, College of Engineering, University of Washington, Seattle, Wash. 98195. He is now with the Department of Biophysics and Bioengineering, University of Utah, Salt Lake City, Utah.

$$a_n{}^t = \frac{j_n(ka)}{j_n(Nka)} + a_n{}^r \frac{h_n{}^{(1)}(ka)}{j_n(Nka)}$$

$$b_n{}^t = \frac{j_n(ka)}{Nj_n(Nka)} + b_n{}^r \frac{h_n{}^{(1)}(ka)}{Nj_n(Nka)}$$

$$a_n{}^r = -\frac{j_n(Nka)[kaj_n(ka)]' - j_n(ka)[Nkaj_n(Nka)]'}{j_n(Nka)[kah_n{}^{(1)}(ka)]' - h_n{}^{(1)}(ka)[Nkaj_n(Nka)]'}$$

$$b_n{}^r = -\frac{j_n(ka)[Nkaj_n(Nka)]' - N^2 j_n(Nka)[kaj_n(ka)]'}{h_n{}^{(1)}(ka)[Nkaj_n(Nka)]' - N^2 j_n(Nka)[kah_n{}^{(1)}(ka)]'}$$

and

$$\boldsymbol{m}_{o1n}{}^{(1)} = j_n(NkR)\frac{P_n{}^1}{\sin\theta}\cos\phi\hat{\boldsymbol{\theta}} - j_n(NkR)\frac{\partial P_n{}^1}{\partial\theta}\sin\phi\hat{\boldsymbol{\phi}}$$

$$\boldsymbol{n}_{e1n}{}^{(1)} = \frac{n(n+1)}{NkR} j_n(NkR) P_n{}^1 \cos\phi\hat{\boldsymbol{r}} + \frac{[NkRj_n(NkR)]'}{NkR}\frac{\partial P_n{}^1}{\partial\theta}\cos\phi\hat{\boldsymbol{\theta}} - \frac{[NkRj_n(NkR)]'}{NkR}\frac{P_n{}^1}{\sin\theta}\sin\phi\hat{\boldsymbol{\phi}}$$

where primes denote differentiation with respect to NkR. $N^2 = \epsilon_1 + i\epsilon_2$ is the relative complex dielectric constant, k is the plane wave propagation constant in the medium surrounding the sphere, R is the spherical radius coordinate, and a is the sphere radius. The complex dielectric constants appropriate for biological tissues are given in Table I for the HF frequencies considered [1], [3].

The radius of a sphere simulating a 70-kg man is approximately 25 cm. In the range 1–20 MHz, the free-space ka factor, the magnitude of the complex refractive index N of most tissues in man, and the magnitude of the Nka factor vary as follows:

$$0.005 < ka < 0.1$$
$$91 > |N| > 23$$
$$0.5 < |Nka| < 2.5.$$

Since ka is always small, we can use the first term of the series for spherical Bessel functions of argument ka expanded about zero, and the coefficients $a_n{}^t$ and $b_n{}^t$ can be obtained. The solutions involve the functions $j_n(Nka)$.

$$a_n{}^t = \frac{n!(2ka)^n}{(2n)!}\{nj_n(Nka) + [Nkaj_n(Nka)]'\}^{-1}$$

$$b_n{}^t = \frac{n!(2ka)^n N}{(2n)!}\{nN^2 j_n(Nka) + [Nkaj_n(Nka)]'\}^{-1}.$$

For the lower frequencies, assuming small Nka, we obtain

$$a_n{}^t = N^{-n} \quad \text{and} \quad b_n{}^t = \frac{2n+1}{nN} a_n{}^t.$$

Thus if $|N|$ is large, the $a_n{}^t$ solution predominates. The $a_n{}^t$ expression is a magnetic-type solution, giving rise to magnetic modes of oscillation in the sphere. The $b_n{}^t$ expression, on the other hand, is an electric-type solution, giving rise to electric modes of oscillation. Since $|N| \gg 1$, the magnetic-type solution predominates in the HF band for a spherical model man. The $n=1$ term is dominant in the HF band; therefore, a reasonable approximation of the fields could be obtained using the $n=1$ term of the series in (1). In fact, for the range of $|Nka|$ values where just the first term in the expression of the spherical Bessel function of argument Nka is valid, the expression reduces to that corresponding to the sum of the quasi-static solutions for a uniform electric and uniform magnetic field impressed on the sphere.

TABLE I
DIELECTRIC PROPERTIES OF BIOLOGICAL TISSUES IN THE HF BAND OF ELECTROMAGNETIC RADIATION

Frequency	Dielectric Constant			
MHz	muscle, skin		fat, bone	
	ϵ_1	ϵ_2	ϵ_1	ϵ_2
1	2000.0	7190.0		
2	668.49	5364.3		
5	202.98	2349.5		
10	160.0	1125.0		
20	132.84	534.6	23.50	13.44
27.12	113.0	405.6	20.0	10.2
40.68	97.3	306.2	14.6	7.86
60	84.5	228.0	10.3	6.18
80	76.0	182.4	8.53	5.80
100	71.7	159.8	7.45	5.44

$$\boldsymbol{E}_t = E_0 e^{-i\omega t}\left[\underbrace{\frac{3}{N^2}\hat{\boldsymbol{x}}}_{\text{quasi-static electric term}} + \underbrace{i\frac{kR}{2}(\cos\phi\hat{\boldsymbol{\theta}} - \cos\theta\sin\phi\hat{\boldsymbol{\phi}})}_{\text{quasi-static magnetic term}}\right]. \quad (2)$$

Notice the electric solution is polarized along the x axis as is the incident wave E field. The field is uniform and identical to the electrostatic solution for a dielectric sphere. Thus as for the case of a dielectric sphere in a static field, a surface polarization is set up which generates a uniform internal field which is independent of sphere size. The magnetic solution is much different in form and an order of magnitude greater in amplitude than the electric solution, and is identical to the quasi-static magnetic solution obtained from $\int \boldsymbol{E}\cdot d\boldsymbol{l} = i\omega\mu\int \boldsymbol{H}\cdot d\boldsymbol{A}$. A sketch of the electric and magnetic solutions shown in Fig. 2 illustrates the field configuration and power absorption pattern. The magnetic solution dominates because of the very high values of tissue permittivity.

Equation (2) evaluated along the z axis gives

$$\boldsymbol{E}_t = E_0 e^{-i\omega t}\left[\frac{3}{\epsilon_1{}^2 + \epsilon_2{}^2}(\epsilon_1 - i\epsilon_2) + i\frac{kz}{2}\right]. \quad (3)$$

This indicates that the power absorption is greater at the leading edge of the sphere. The time-average density $\overline{W}_L$ inside the spherical model can be obtained from the relation

$$\overline{W}_L = \tfrac{1}{2}\sigma \boldsymbol{E}_t\cdot\boldsymbol{E}_t^* \quad (4)$$

where * denotes complex conjugate and $\sigma = \omega\epsilon_0\epsilon_2$ is the electrical conductivity. This results in

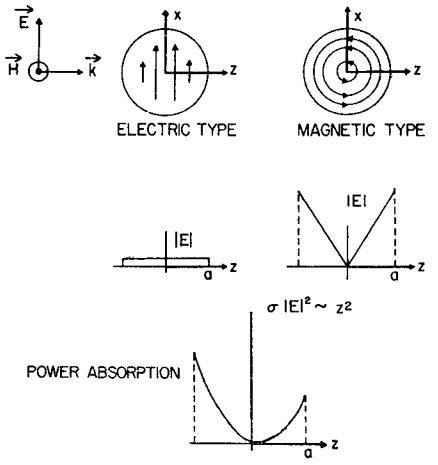

Fig. 2. Electric-field and power absorption patterns given by the quasi-static electric and induced magnetic solutions.

$$\overline{W}_L = \tfrac{1}{2}\sigma E_0^2 \left[\frac{9}{\epsilon_1^2 + \epsilon_2^2} - \frac{3\epsilon_2 kR\cos\theta}{\epsilon_1^2 + \epsilon_2^2} + \left(\frac{kR}{2}\right)^2 (\cos^2\phi + \cos^2\theta \sin^2\phi) \right]. \quad (5)$$

Integration of $\overline{W}_L$ over the sphere volume gives the total time-average absorbed power W_t from which average absorbed power per unit weight can be calculated:

$$W_t = \tfrac{1}{2}\sigma E_0^2 \frac{4\pi a^3}{3} \left[\underset{\substack{\uparrow \\ \text{quasi-static} \\ \text{electric term}}}{\frac{9}{\epsilon_1^2 + \epsilon_2^2}} + 0.4 \underset{\substack{\uparrow \\ \text{quasi-static} \\ \text{magnetic term}}}{\left(\frac{ka}{2}\right)^2} \right]. \quad (6)$$

It is interesting to note again that the total absorbed power in the sphere is the additive sum of the quasi-static electric component and the quasi-static magnetic component.

The physical insight gained from recognizing that the total electric field inside the sphere and the total absorbed power are given by the sum of quasi-static electric and magnetic solutions makes it possible to infer the effects of absorbed power by impressed fields of variable E/H ratio such as in the near field of an HF antenna. Defining the impedance ratio as $\eta = (Ex/Hy)/\eta_0$, where $\eta_0 = 120\pi\,\Omega$, the field equation of (2) becomes simply

$$E_t' - E_0 e^{-i\omega t} \left[\frac{3}{N^2}\hat{x} + i\frac{kR}{2\eta}(\cos\phi\hat{\theta} - \cos\theta\sin\phi\hat{\phi}) \right] \quad (7)$$

and the total time-average absorbed power is given by

$$W_t' = \tfrac{1}{2}\sigma E_0^2 \frac{4\pi a^3}{3} \left[\frac{9}{\epsilon_1^2 + \epsilon_2^2} + 0.4\left(\frac{ka}{2\eta}\right)^2 \right]. \quad (8)$$

Power Deposition and Induced Field Distribution

Whole Body

In order to quantify the power deposition from an HF EM field and the internal distribution in a human body as a function of frequency and field type, a homogeneous sphere of muscle material is chosen. The total radius of the sphere is taken as 25.57 cm., which has the mass corresponding to a man weighing 70 kg. An incident power of 1 mW/cm² is assumed throughout.

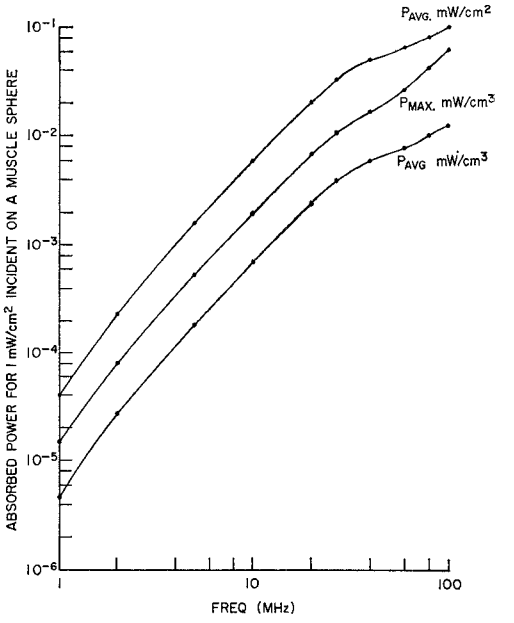

Fig. 3. Absorbed power characteristics for a man-size sphere in a plane wave HF field.

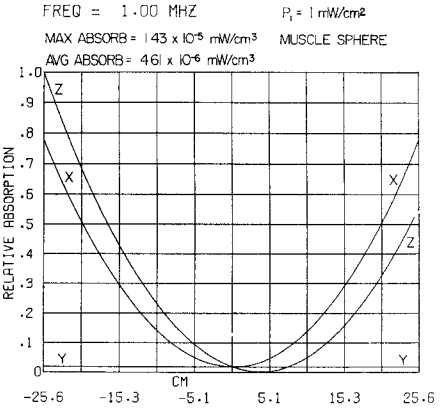

Fig. 4. Absorbed power distributions along the x, y, and z axes of a man-size homogeneous muscle sphere in a plane wave HF field. The propagation is along the z axis; polarization is in the x direction.

The maximum or peak absorbed power per unit volume, the average absorbed power per unit volume, and the average absorbed power per unit surface area as a function of frequency are shown in Fig. 3. Note that the absorbed power densities increase monotonically with the square of frequency within the HF band.

The spatial distributions of the absorbed power are shown in Fig. 4. In each of these graphs, the patterns are normalized to the maximum along any one of the three orthogonal rectangular coordinate axes. Though the absorbed powers differ greatly for different frequencies, the spatial distributions of the absorbed power inside the spheres are quite similar. The maximum absorption occurs always at the leading surface, while absorption at the trailing surface is 0.5–0.7 times the maximum value. The toroidal pattern is governed mainly by the dominant role of the magnetically induced component of absorbed power. The absorbed power in the center of the

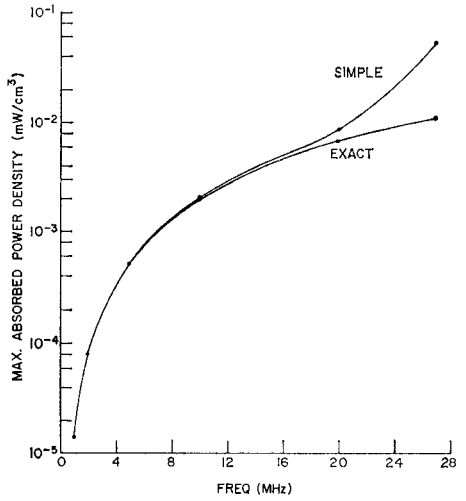

Fig. 5. Maximum absorbed power densities in a man-size sphere given by exact Mie solution and the simplified solution. Incident power density is 1 mW/cm².

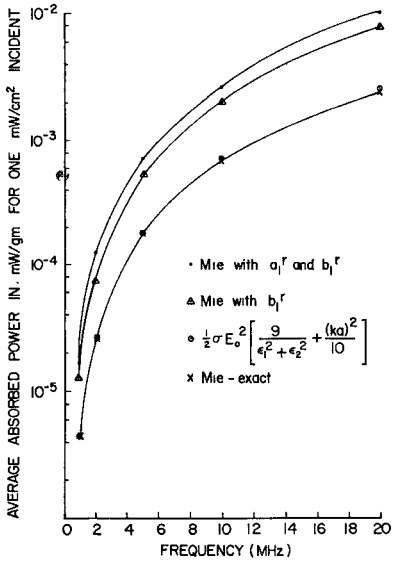

Fig. 6. Average power absorption by a 25.57-cm-radius muscle sphere in a 1-mW/cm² incident plane wave field; a comparison of theoretical predictions.

sphere, however, is due solely to the electrically induced component. To estimate the validity and range of applicability of this simple solution, the maximum absorbed power densities are calculated from this solution and compared with the exact Mie results in Fig. 5 [12]. Within the HF band, the difference in the two solutions is quite small. For example, at 20 MHz the difference is about 20 percent, and as the frequency is decreased below 16 MHz, the difference becomes negligible. The average absorbed power comparisons between that calculated from (6) and the exact are shown in Fig. 6. Also shown on Fig. 6 are the results of absorbed power calculated using scattering parameters, taking into account both first-order electric and magnetic oscillations and taking only the first-order electric oscillation into consideration. The latter has been used to obtain average power absorption in the past [9], [10]. The spatial distributions of the absorbed power along the z axis calculated from (5) are shown in Fig. 7. The close agreement suggests that the simplified solution can be applied with confidence to all frequencies within the HF band for a conservative estimate of absorption of EM power by the spherical man.

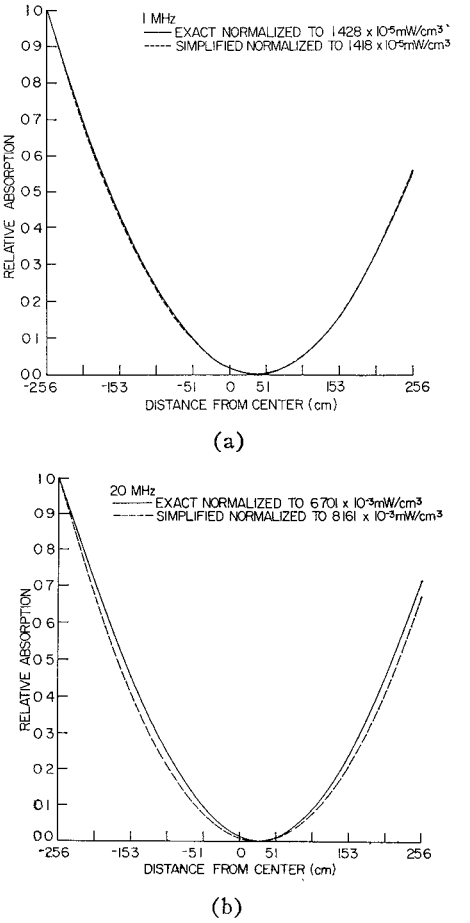

Fig. 7. Normalized absorbed power distributions calculated from the exact Mie solution and the simplified solution. Incident power density is 1 mW/cm².

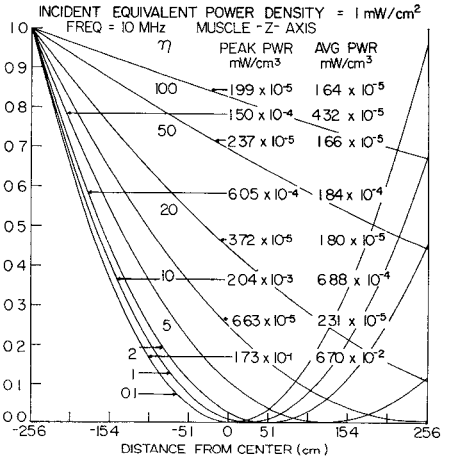

Fig. 8. Power absorption and distribution as a function of normalized impedance.

Calculations of the absorbed power along the z axis and x axis for a 25.57-cm-radius muscle sphere using (7) and (8) are shown in Fig. 8 and Fig. 9 for variable real values of η. For predominantly magnetic fields (η small) the absorption becomes much more intense and proportional to z^2 or x^2, whereas for predominantly electric fields (η large), the ab-

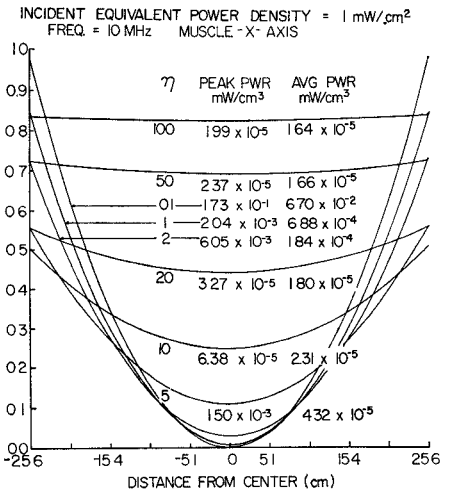

Fig. 9. Power absorption and distribution as a function of normalized impedance.

TABLE II
DIELECTRIC PROPERTIES OF BRAIN MATERIAL

Frequency	Relative Dielectric Constant	
Hz	ϵ_1	ϵ_2
10	6,568,085	122,899,055
10^2	525,447	13,235,546
10^3	85,385	1,477,152
10^4	39,408	153,624
10^5	13,136	22,452
10^6	953	4,727
10^7	105	739
10^8	43	95.8
9.15×10^8	34.42	15.49
2.45×10^9	30.87	10.65
10^{10}	24.23	15.2

Note: Values at 100 MHz and below are extrapolated from the following formula: $\epsilon_b = [(\epsilon_b(2450)/(\epsilon_m(2450))]/\epsilon_m$, where ϵ_b and ϵ_m are the values at the frequency of interest for brain and muscle, and ϵ_b (2450) and ϵ_m (2450) are the values for brain and muscle at 2450 MHz. as given by Schwan *et al.* [1], [3].

sorbed power is reduced and approaches the uniform absorption pattern of the quasi-static electric solution.

The implications of this result are significant with regard to the estimation of HF hazards from survey meters which sense only E fields. It is the magnetic fields which are the primary sources of absorbed power for $10 > \eta > 0$, and these need to be measured to obtain any kind of estimate of HF hazard.

Brain

With the large number of reports alluding to central nervous system (CNS) effects of EM fields, it is of interest to investigate the absorption properties of a human head exposed to HF fields. The dielectric properties of brain matter as a function of frequency are given in Table II. Though the

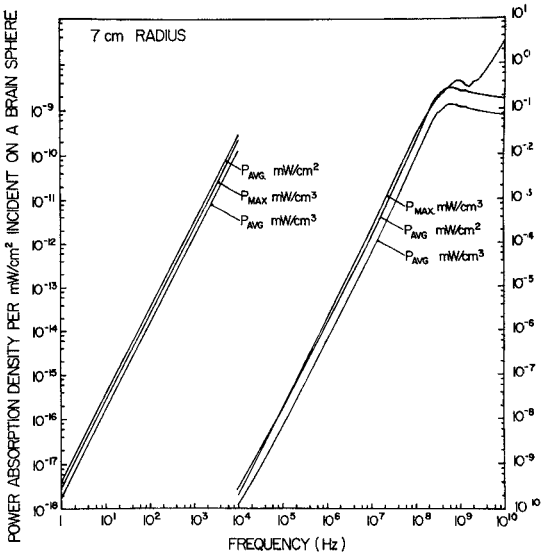

Fig. 10. Absorbed power characteristics for a spherical head model exposed to plane wave HF field.

human head covers a wide range of sizes, a sphere of radius 7 cm is assumed here. The *Nka* factors for a 7-cm brain at 10 and 100 MHz are

$$|Nka| = 1.50, \quad \text{at 100 MHz}$$
$$|Nka| = 0.40, \quad \text{at 10 MHz.}$$

Therefore, (2) and (6) apply, respectively, for the induced field distribution inside the head and the total time-average absorbed power for 100 MHz and below; above 100 MHz, (1) must be used. This conclusion has also been borne out by comparing the computed results using the approximate equations (2) and (6) with that of the exact equation (1). The power absorption density in the head exposed to an incident flux of 1 mW/cm² is shown in Fig. 10. Notice that for frequencies below 100 MHz the absorption behaves as f^2 and, in general, is an order of magnitude smaller than the corresponding absorption for the whole body model (see Fig. 3). The distributions of the absorbed power density inside the brain shown in Fig. 11 are similar to that of the whole body. The only difference is that, in this case, the absorption by the leading surface is much higher than that at the trailing surface. This results from the change in relative magnitude and phase between the electric fields induced in the sphere by the incident electric and magnetic fields.

Effect of Body Size on HF Power Absorption

Equations (3), (5), and (6) indicate that the power absorption and distribution inside a subject are functions of size. Specifically, the size dependence is governed mainly by the magnetically induced field component, since the electrical coupling is independent of size. It is conceivable, then, that for sufficiently small subjects, the role of incident electric and magnetic fields in producing predominate absorption inside a subject may reverse. To investigate this, a muscle sphere with a 1.68-cm radius is used to simulate a 20-g mouse. The maximum power absorption in a mouse-size sphere due to a 1-mW/m² incident plane wave has been calculated and compared to that absorbed by a man-size sphere (Fig. 12). The maximum absorptions corresponding to a 61.4-V/m applied electric field and a 0.163-A/m applied magnetic field are also

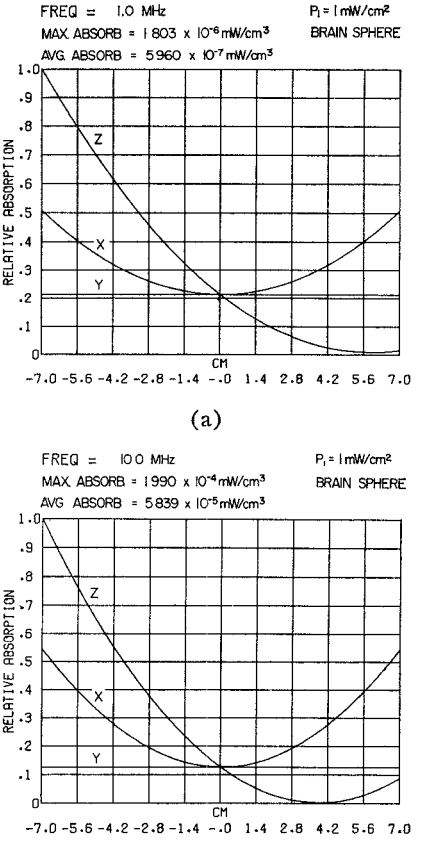

Fig. 11. Absorbed power distributions along the x, y, and z axes of a homogeneous spherical model of human brain exposed to plane wave HF field.

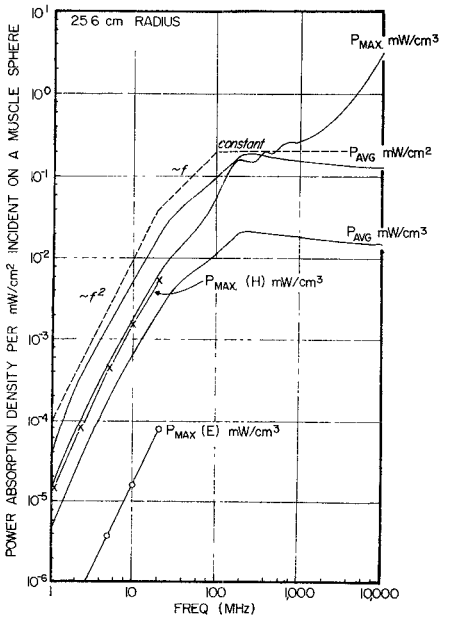

Fig. 12. Frequency dependence of absorbed power by a man-size sphere in a 1-mW/cm² plane wave P, 61.4-V/m electric field $P(E)$, and 0.163-A/m magnetic field $P(H)$.

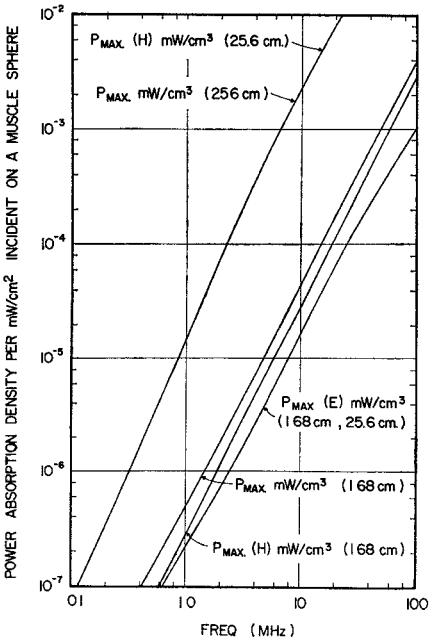

Fig. 13. Effect of body size on the absorption of 1-mW/cm² HF plane wave P, 61.4-V/m electric field $P(E)$, and 0.163-A/m magnetic field $P(H)$.

shown on the figure. It can be seen that the magnetically induced absorption in man can be two orders of magnitude greater than the electric component. The absorption in the mouse-size sphere due to electric and magnetic coupling is on the same order of magnitude in the HF range, and the electric coupling tends to dominate as the frequency is reduced. This indicates that one must be discrete in drawing conclusions about human exposures from animal results.

Conclusions

Simple analytic expressions for the induced field in a man-size homogeneous sphere and the total power absorption have been obtained in an HF field. The results indicate that for field impedance magnitude less than $1200\pi\ \Omega$, magnetic coupling is far more important than electric coupling at HF frequencies and below. Moreover, it has been shown that the induced field and the total absorbed power can be obtained from the sum of quasi-static electric and magnetic solutions for frequencies below 20 MHz. The power absorption decreases sharply as the frequency is reduced. Fig. 13 illustrates the frequency dependence of the absorbed power density for incident plane wave, and applied electric and magnetic fields. The curves show that below 100 MHz the power absorption falls off directly with frequency to about 20 MHz and as the square of frequency thereafter. It is therefore clear that the coupling of EM energy to the human body is much reduced at HF frequencies and below as compared with the microwave range.

The close agreement between the approximate expressions and the exact Mie theory suggests that the simplified solution can be applied with confidence to frequencies in the HF band and lower for a conservative estimate of the EM power absorption by a man-size sphere. The study also indicates that it is necessary to measure both the electric and magnetic fields in order to assess the biological hazard of HF field exposure. The relative significance of applied electric and magnetic

fields in producing power absorption in various subjects differs according to their sizes.

References

[1] C. C. Johnson and A. W. Guy, "Nonionizing electromagnetic wave effects in biological materials and systems," *Proc. IEEE*, vol. 60, pp. 692–718, June 1972.

[2] S. M. Michaelson, "Human exposure to nonionizing radiant energy—Potential hazards and safety standards," *Proc. IEEE*, vol. 60, pp. 389–421, Apr. 1972.

[3] A. S. Pressman, *Electromagnetic Fields and Life* (translated from Russian). New York: Plenum, 1970.

[4] K. Martha, J. Musil, and H. Tuha, *Electromagnetic Fields and the Environment* (translated from Czech). San Francisco, Calif.: San Francisco Press, 1971.

[5] "Biological effects and health implications of microwave radiation," in *Symp. Proc.*, S. F. Cleary, Ed., BRH–DBE 70-2, U. S. Department of Health, Education, and Welfare, Rockville, Md., Sept. 17–19, 1969.

[6] *IEEE Trans. Microwave Theory Tech. (Special Issue on Biological Effects of Microwaves)*, vol. MTT-19, pp. 128–257, Feb. 1971.

[7] R. A. Tell, "Broadcast radiation: How safe is safe?" *IEEE Spectrum*, vol. 9, pp. 43–51, Aug. 1972.

[8] H. R. Kucia, "Accuracy limitations in measurements of HF field intensities for protection against radiation hazards," *IEEE Trans. Instrum. Meas. (1972 Conference on Precision Electromagnetic Measurements)*, vol. IM-21, pp. 412–415, Nov. 1972.

[9] S. J. Rogers, "Radio frequency radiation hazards to personnel at frequencies below 30 MHz," in *Symp. Proc. Biological Effects and Health and Implications of Microwave Radiation* (Richmond, Va.), Sept. 17–19, 1969, pp. 222–232.

[10] H. P. Schwan, "Biological hazards from exposure to ELF electrical fields and potentials," U. S. Naval Weapons Lab., Tech. Rep. TR-2713, Mar. 1972.

[11] J. A. Stratton, *Electromagnetic Theory*. New York: McGraw-Hill, 1941, sec. 9.25.

[12] A. W. Guy, C. C. Johnson, J. C. Lin, A. F. Emery, and K. K. Kraning, "Electromagnetic power deposition in man exposed to HF fields and the associated thermal and physiological consequences," Univ. Washington School of Medicine, Dep. Rehabilitation Medicine, Seattle, Sci. Rep. 1, Mar. 1973.

Characterization of Nonlinearities in Microwave Devices and Systems

GEORGE L. HEITER, MEMBER, IEEE

Invited Paper

***Abstract*—A simple model to describe a nonlinear device or system is proposed which extends the power series expansion, conventionally restricted to amplitude nonlinearities, to include phase nonlinearities as well. Four different test methods are selected for which the experimentally observed nonlinearity parameters are related to the "gain" and "phase" coefficients of the extended series. A set of simplified relationships is derived where the "1-dB gain compression point" represents gain contributions only while phase nonlinearities are included in the "intercept point," the "third-order intermodulation (IM) coefficients," and the "noise-power-ratio (npr)." For a TWT amplifier in which phase nonlinearities dominate, the third-order IM coefficient was measured. The results are compared with those calculated from single-tone and noise-loading tests using the relationships derived from the model. Agreement to ±1 dB is found over a 15-dB power range.**

I. Introduction

With microwave devices and systems utilized ever closer to their limits, linear measurement techniques are no longer sufficient to describe final performance under multisignal loading conditions. As a result, a number of techniques have evolved which are used to characterize nonlinear behavior and the resulting intermodulation (IM) performance. Selection of a particular technique depends on the type of information desired, such as detailed diagnostic information on the origin of nonlinearity, overall IM performance under different loading conditions, etc. Four of these techniques—single-tone, two-tone, three-tone testing, and noise loading—were discussed at a panel session [1] on which this paper is based.

Some of the present microwave techniques have been adapted from the CATV industry [1, p. 112], [3] where the IM performance at UHF frequencies has been a primary concern for about two decades. There it has been found that the reliability of IM testing for system evaluation increases as the probing signal spectrum approaches that of the actual system load.

The usefulness of tests with probing signals which have a spectral distribution different from that of the final system load depends in part on how closely the selected mathematical model approaches actual device behavior. The Volterra series expansion [3]–[6] allows detailed and accurate representation of device characteristics, including memory, which can be applied directly to any spectral distribution of the system load. Measurement [6] of the relevant parameters (kernels), however, is sometimes time consuming and may exceed available measurement capabilities.

In this paper a simple mathematical model is proposed which is used to describe the amplitude and phase nonlinearities (gain deviation and AM–PM conversion) observed in microwave devices. From this model the parameters relevant to each of the four measurement techniques are derived and interrelated (equation numbers of simplified relationships are marked □ for convenient reference). For each technique

Manuscript received August 14, 1973; revised August 29, 1973.
The author is with Bell Laboratories, North Andover, Mass. 01845.